Title: From plants to minerals: depth-dependent controls on microbial carbon use efficiency across the global

Yaqin Guo [a, b], Yongxing Cui [a, b*], Tessa Camenzind [a, c], Matthias C. Rillig [a, b]

[a] Institute of Biology, Freie Universität Berlin, Altensteinstraße 6, 14195 Berlin, Germany

[b] Berlin-Brandenburg Institute of Advanced Biodiversity Research (BBIB), Berlin, Germany

[c] Department of Soil Biology, University of Hohenheim, Emil-Wolff-Straße 27, 70593 Stuttgart, Germany

Contents of this file:

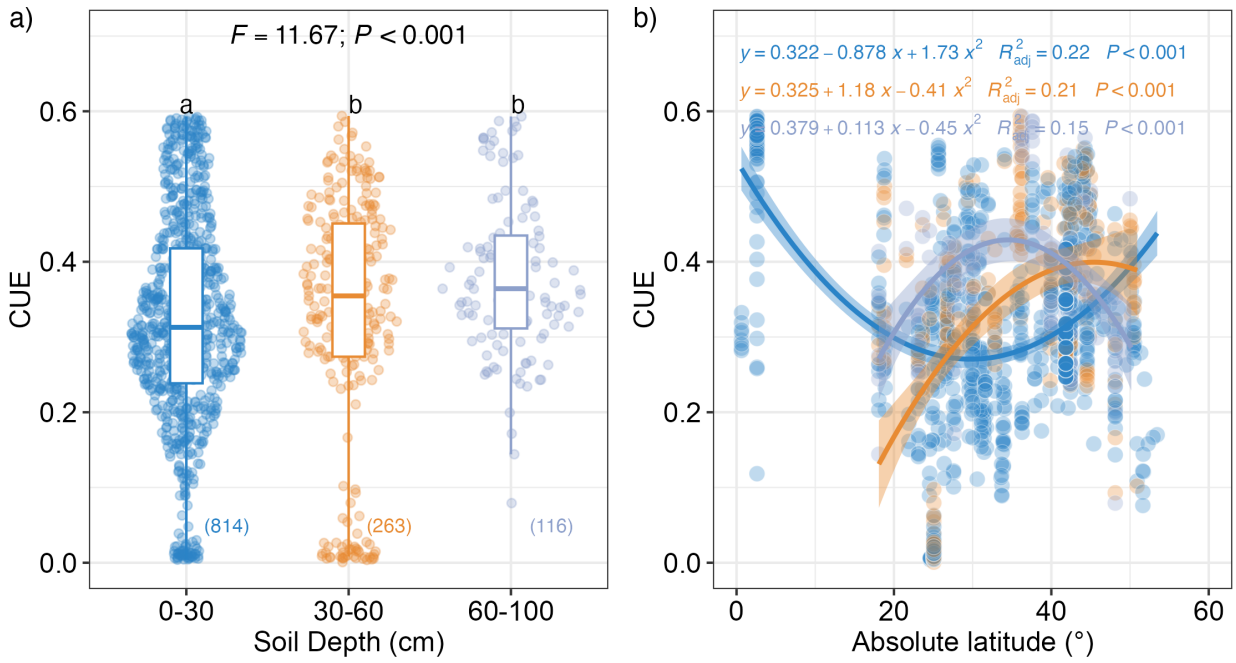

Fig. S1 a) Differences in CUE among 0-30 cm, 30-60 cm, and 60-100 cm. Mean values are 0.35 (0.31-0.38), 0.37 (0.33-0.41), and 0.38 (0.34-0.42), respectively. The boxes represent the first and the third quartiles. The line within the box represents the median. The whiskers represent the data range and points indicate individual values. Different letters denote significant differences ($P < 0.05$) based on the analysis of linear mixed-effect models followed by estimated marginal means test. b) Latitudinal patterns of CUE fitted by quadratic models in three layers, respectively. Formulars and adjust coefficient were annotated in the plot; $P < 0.001$ indicate statistically significant of the overall regression model.

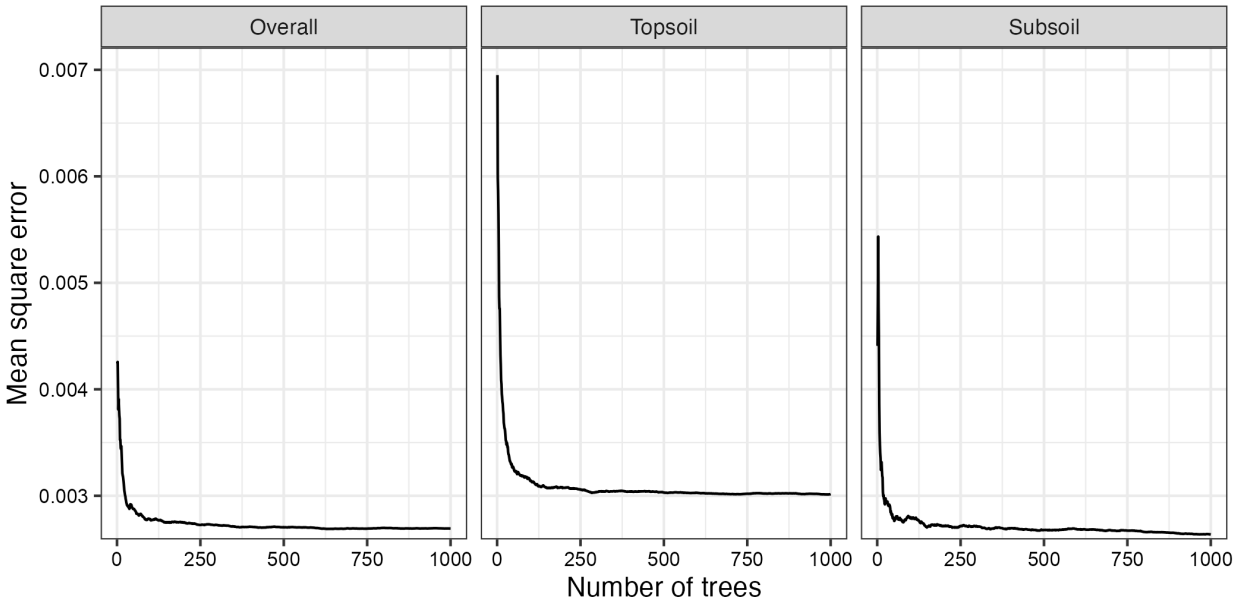

Fig. S2 Changes in the mean squared error of predicted values with the number of regression trees in random forest modeling based on sampling sites. The curves, which steadily approach the horizontal, indicating that 1000 regression trees are sufficient for structuring prediction models. Note: Overall means topsoils and subsoils together.

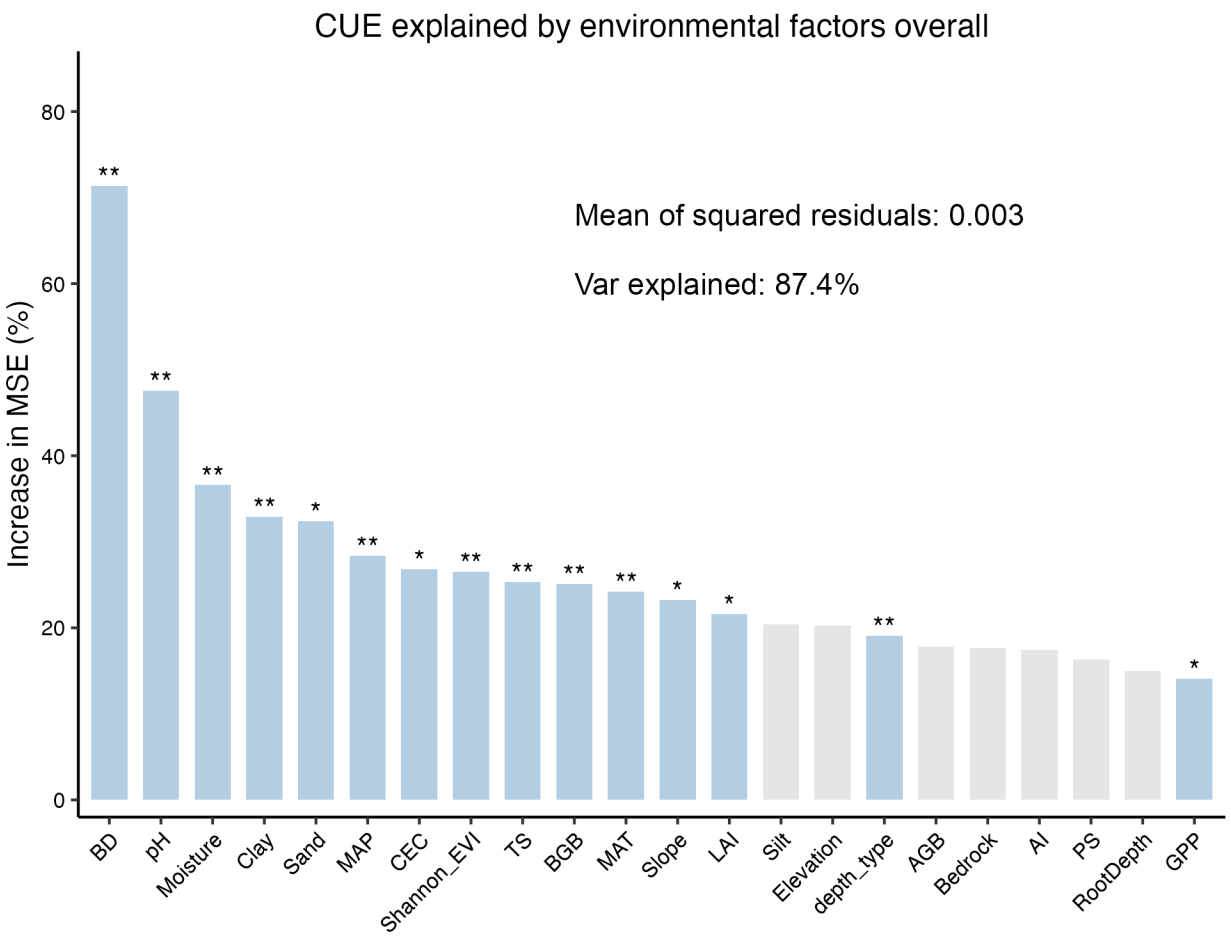

Fig. S3 Random Forest analysis identifies important variables when combined both topsoils and subsoils named as overall. MAT: mean annual temperature; MAP: mean annual precipitation; TS: temperature seasonality; PS: precipitation seasonality; AI: aridity index; GPP: gross primary production; LAI: leaf area index; AGB: aboveground biomass; BGB: belowground biomass; BD: bulk density; CEC: cation exchange capacity.

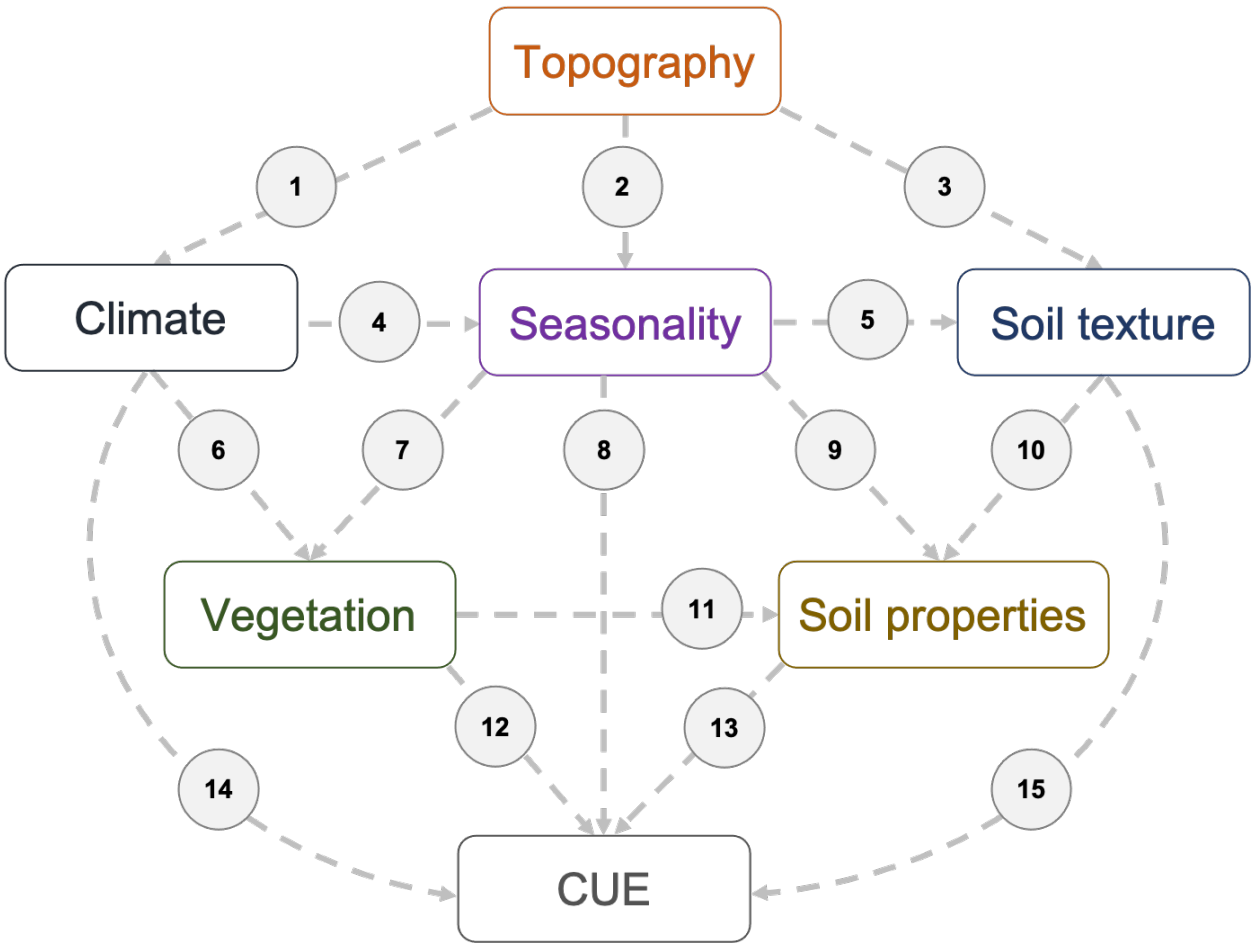

#	Factor	Rationale
1	Topography → Climate	Topography influences local climate by altering temperature and precipitation patterns. Temperature typically decreases by about 6.5˚C for every 1,000 m increase in elevation due to adiabatic cooling, while higher elevations and steeper, windward slopes often receive more precipitation because of orographic uplift.
2	Topography → Seasonality	Topography affects climate seasonality by enhancing thermal and moisture contrasts. Higher elevations show greater temperature seasonality due to stronger radiative cooling, while elevation and slope increase precipitation seasonality through intensified orographic uplift during wet seasons.
3	Topography → Soil texture	Topography is a crucial factor influencing soil clay content, as it governs weathering intensity, erosion, and sediment deposition. Higher elevations and steeper slopes usually have coarser soils due to greater erosion, while lower elevations and gentle slopes accumulate finer materials.
4	Climate → Seasonality	Climate strongly affects seasonality patterns. Regions with higher MAT show lower temperature seasonality, while cooler area experience greater variation. Similarly, regions with higher MAP tend to have more evenly distributed rainfall, whereas drier climates exhibit stronger wet-dry seasonality.
5	Seasonality → Soil texture	Seasonality affects soil clay content by regulating weathering and erosion. For example, strong temperature and precipitation seasonality enhance weathering and runoff, reducing clay formation.

6	Climate → vegetation	Climate is a primary determinant of vegetation distribution and productivity. Higher MAT promotes plant growth where moisture is adequate, while MAP determines water availability and vegetation density.
7	Seasonality → Vegetation	Climate seasonality greatly affects the growth, reproduction, and survival of plants by periodic changes in temperature and precipitation.
8	Seasonality → CUE	Seasonality can influence temperature and moisture variations, thus shaping microbial use efficiency.
9	Seasonality → Soil properties	Seasonality influences soil properties such as pH and BD by controlling moisture and temperature fluctuations that affect leaching, organic matter decomposition, and soil structure.
10	Soil texture → Soil properties	Soil clay or sand content strongly influences pH, DB and water holding capacity by affecting ion exchange capacity, porosity, and soil structure.
11	Vegetation → Soil properties	Vegetation can influence soil properties via root exudates, litter input. For example, BD is strongly related to organic matter.
12	Vegetation → CUE	Vegetations strongly influence microbial CUE by regulating the quantity and quality of organic carbon inputs to the soil.
13	Soil properties → CUE	Soil properties strongly regulate microbial CUE by influencing nutrient availability, aeration, and habitat conditions.
14	Climate → CUE	Climate will change temperature and moisture adaptation of microbial communities, thereby influencing microbial carbon use efficiency.
15	Soil texture → CUE	Different clay or sand content will affect substrate absorption and accessibility, thus affecting carbon use efficiency.

Fig. S4 A *priori* path model (modified from the framework in (Cui et al. 2025)) illustrating the direct and indirect effects of key environmental factors on soil microbial carbon use efficiency (CUE). In our study, we employed the same modeling to test the casual relationships between environmental factors and CUE in both topsoils and subsoils. While topsoils and subsoils are subject to the same topography, climate, seasonality, and vegetation influences, they may differ in their responses due to variations in soil buffer capacity rather than in exposure to different climate conditions. Although we acknowledge potential differences in plant carbon (C) allocation to subsoils, our analysis focuses on overall ecosystem productivity. The estimation of C allocation to subsoils could be approached by the available model (Luo et al. 2019), but their accuracy is limited by insufficient empirical data for robust parameterization. MAT: mean annual temperature; MAP: mean annual precipitation; BD: bulk density.

Table S1 Detailed results of path analysis modeling on a global scale in topsoils

MODEL SPECIFCATION

1	Number of Cases	814
2	Latent Variables	7
3	Manifest Variables	15
4	Scale of Data	Standardized Data
5	Non-Metric PLS	FALSE
6	Weighting Scheme	centroid
7	Tolerance Crit	1e-06
8	Max Num Iters	100
9	Convergence Iters	6
10	Bootstrapping	FALSE
11	Bootstrapping samples	NULL

BLOCK DEFINITION

	Block	Type	Size	Mode
1	Topography	Exogenous	2	A
2	Climate	Endogenous	2	A
3	Season	Endogenous	2	A
4	Soil texture	Endogenous	1	A
5	Vegetation	Endogenous	3	B
6	Soil properties	Endogenous	3	B
7	CUE	Endogenous	1	A

BLOCKS UNIDIMENSIONALITY

	Mode	MVs	C.alpha	DG.rho	eig.1st	eig.2nd
Topography	A	2	0.641	0.848	1.470	0.529
Climate	A	2	0.770	0.897	1.630	0.374
Season	A	2	0.866	0.937	1.760	0.237
Soil texture	A	1	1.000	0.000	1.500	0.499
Vegetation	B	3	0.000	0.000	1.690	1.003
Soil properties	B	3	0.000	0.000	1.180	1.027
CUE	A	1	1.000	1.000	1.000	0.000

OUTER MODEL

		Weight	Loading	Communality	Redundancy
topography					
1	Elevation	0.962	0.998	0.996	0.000
1	Slope	0.067	0.523	0.273	0.000
climate					
2	MAT	0.610	0.921	0.850	0.184
2	MAP	0.497	0.880	0.773	0.168
season					
3	PS	0.502	0.931	0.868	0.706
3	TS	0.563	0.946	0.895	0.728
texture					
4	Clay	0.705	-0.925	0.855	0.329
4	Sand	0.563	0.946	0.895	0.728
vegetation					
5	GPP	0.901	0.994	0.988	0.593
5	BGB	0.117	0.483	0.233	0.140
5	Shannon_EVI	-0.08	-0.581	0.337	0.202
soil					
6	BD	-0.021	0.061	0.004	0.001
6	pH	1.008	-0.994	0.989	0.228

6	Moisture	0.101	0.036	0.001	0.000
CUE					
7	CUE	1.000	1.000	1.000	0.222

CROSSLOADINGS

		topography	climate	season	texture	vegetation	soil	CUE
topography								
1	Elevation	0.998	-0.478	0.142	0.318	-0.349	-0.259	-0.164
1	Slope	0.523	-0.057	-0.108	0.117	-0.154	0.182	-0.296
climate								
2	MAT	-0.460	0.922	-0.831	-0.544	0.762	0.311	0.112
2	MAP	-0.372	0.880	-0.688	-0.433	0.594	0.566	0.112
season								
3	PS	0.193	-0.746	0.932	0.502	-0.569	-0.363	-0.065
3	TS	0.058	-0.846	0.946	0.566	-0.778	-0.343	-0.144
texture								
4	Clay	-0.301	0.539	-0.554	0.502	-0.569	-0.363	-0.065
4	Sand	0.234	-0.381	0.409	0.566	-0.778	-0.343	-0.144
vegetation								
5	GPP	-0.338	0.772	-0.729	-0.663	0.994	0.398	0.321
5	BGB	-0.001	0.183	-0.284	-0.494	0.483	0.580	0.032
5	Shannon_EVI	0.517	-0.527	0.410	0.408	-0.581	-0.102	-0.258
Soil								
6	BD	-0.250	0.343	-0.150	0.054	0.066	0.061	0.080
6	pH	0.201	-0.447	0.371	0.436	-0.414	-0.994	0.115
6	Moisture	0.295	-0.131	-0.021	0.027	-0.161	0.036	-0.215
CUE								
7	CUE	-0.179	0.124	-0.113	-0.302	0.314	-0.093	1.000

INNER MODEL

$climate				
	Estimate	Std. Error	t value	Pr(>|t|)
Intercept	-1.08e-15	0.031	-3.49e-14	1.00e+00
topography	-4.66e-01	0.031	-1.50e+01	4.19e-45
$season				
	Estimate	Std. Error	t value	Pr(>|t|)
Intercept	-1.06e-15	0.015	-6.99e-14	1.00e+00
topography	-3.40e-01	0.017	-1.98e+01	1.19e-71
climate	-1.01e+00	0.017	-5.88e+01	1.18e-294
$texture				
	Estimate	Std. Error	t value	Pr(>|t|)
Intercept	-8.12e-17	0.028	-2.95e-15	1.00e+00
topography	2.45e-01	0.029	8.81e+00	7.46e-18
season	5.39e-01	0.029	1.94e+01	4.32e-69
$vegetation				
	Estimate	Std. Error	t value	Pr(>|t|)
Intercept	7.51e-16	0.022	3.38e-14	1.00e+00
climate	5.25e-01	0.042	1.24e+01	1.20e-32
season	-2.78e-01	0.042	-6.59e+00	8.16e-11
$soil				
	Estimate	Std. Error	t value	Pr(>|t|)
Intercept	-4.76e-16	0.031	-1.54e-14	1.00e+00
season	-8.88e-02	0.045	-1.97e+00	4.95e-02
texture	-2.57e-01	0.043	-5.97e+00	3.59e-09

vegetation	1.94e-01	0.051	3.78e+00	1.66e-04
$CUE				
	Estimate	Std. Error	t value	Pr(>|t|)
Intercept	-3.58e-16	0.031	-1.15e-14	1.00e+00
climate	-2.30e-02	0.067	-3.46e-01	7.30e-01
season	2.27e-01	0.062	3.69e+00	2.41e-04
texture	-2.78e-01	0.045	-6.24e+00	7.01e-10
vegetation	4.39e-01	0.056	7.89e+00	1.01e-14
soil	-3.10e-01	0.037	-8.47e+00	1.13e-16

CORRELATIONS BETWEEN LVs

	Topography	Climate	Season	Texture	Vegetation	Soil	CUE
Topography	1.000	-0.466	0.130	0.315	-0.347	-0.238	-0.179
Climate	-0.466	1.000	-0.848	-0.547	0.761	0.471	0.124
Season	0.130	-0.850	1.000	0.571	-0.724	-0.375	-0.113
Texture	0.315	-0.547	-0.553	1.000	-0.689	-0.441	-0.302
Vegetation	-0.347	0.761	0.358	-0.689	1.000	0.435	0.314
Soil	-0.237	0.471	-0.626	-0.441	-0.434	1.000	-0.093
CUE	-0.179	0.124	-0.113	-0.302	0.314	-0.093	1.000

SUMMARY INNER MODEL

	Type	R_2	Block_Communality	Mean_Redundancy	AVE
Topography	Exogenous	0.000	0.635	0.000	0.635
Climate	Endogenous	0.217	0.812	0.176	0.812
Season	Endogenous	0.813	0.881	0.717	0.881
Texture	Endogenous	0.384	0.742	0.285	0.742
Vegetation	Endogenous	0.600	0.519	0.312	0.000
Soil	Endogenous	0.230	0.331	0.076	0.000
CUE	Endogenous	0.222	1.000	0.222	1.000

GOODNESS-OF-FIT
[1] 0.505

TOTAL EFFECTS

	relationships	direct	indirect	total
1	topography -> climate	-0.466	0.000	-0.466
2	topography -> season	-0.340	0.470	0.130
3	topography -> texture	0.245	0.070	0.315
4	topography -> vegetation	0.000	-0.281	-0.281
5	topography -> soil	0.000	-0.147	-0.147
6	topography -> CUE	0.000	-0.125	-0.125
7	climate -> season	-1.009	0.000	-1.009
8	climate -> texture	0.000	-0.543	-0543
9	climate -> vegetation	0.525	0.280	0.805
10	climate -> soil	0.000	0.385	0.385
11	climate -> CUE	-0.023	0.156	0.133
12	season -> texture	0.539	0.000	0.539
13	season -> vegetation	-0.278	0.000	-0.278
14	season -> soil	-0.089	-0.192	-0.281
15	season -> CUE	0.227	-0.185	0.043
16	texture -> vegetation	0.000	0.000	0.000

17	texture -> soil	-0.257	0.000	-0.257
18	texture -> CUE	-0.278	0.080	-0.198
19	vegetation -> soil	0.194	0.000	0.194
20	vegetation -> CUE	0.440	-0.060	0.380
21	soil -> CUE	-0.310	0.000	-0.310

Table S2 Detailed results of path analysis modeling on a global scale in subsoils

MODEL SPECIFCATION

1	Number of Cases	379
2	Latent Variables	7
3	Manifest Variables	15
4	Scale of Data	Standardized Data
5	Non-Metric PLS	FALSE
6	Weighting Scheme	centroid
7	Tolerance Crit	1e-06
8	Max Num Iters	100
9	Convergence Iters	7
10	Bootstrapping	FALSE
11	Bootstrapping samples	NULL

BLOCKDEFINITION

	Block	Type	Size	Mode
1	Topography	Exogenous	2	A
2	Climate	Endogenous	2	A
3	Season	Endogenous	2	A
4	Texture	Endogenous	1	A
5	Vegetation	Endogenous	3	B
6	Soil	Endogenous	3	B
7	CUE	Endogenous	1	A

BLOCKS UNIDIMENSIONALITY

	Mode	MVs	C.alpha	DG.rho	eig.1st	eig.2nd
Topography	A	2	0.256	7.29e-01	1.150	0.853
Climate	A	2	0.929	9.66e-01	1.870	0.133
Season	A	2	0.793	8.84e-01	1.590	0.414
Texture	A	1	0.000	2.36e-32	1.480	0.522
Vegetation	B	3	0.000	0.00e+00	1.250	1.128
Soil	B	3	0.000	0.00e+00	1.260	0.925
CUE	A	1	1.000	1.00e+00	1.000	0.000

OUTER MODEL

		Weight	Loading	Communality	Redundancy
topography					
1	Elevation	0.602	0.707	0.500	0.000
1	Slope	0.715	0.803	0.645	0.000
climate					
2	MAT	0.523	0.967	0.935	0.015
2	MAP	0.512	0.965	0.932	0.015
season					
3	PS	0.434	0.833	0.695	0.015
3	TS	0.682	0.936	0.932	0.015

texture					
4	Clay	0.787	-0.952	0.907	0.051
4	Sand	-0.347	0.723	0.522	0.030
vegetation					
5	GPP	0.832	0.917	0.841	0.542
5	BGB	0.417	0.491	0.241	0.155
5	Shannon_EVI	-0.152	-0.212	0.045	0.029
soil					
6	BD	-0.111	0.240	0.058	0.035
6	pH	0.982	-0.993	0.986	0.591
6	Moisture	0.060	0.033	0.001	0.001
CUE					
7	CUE	1.000	1.000	1.000	0.388

CROSSLOADINGS

		topography	climate	season	texture	vegetation	soil	CUE
topography								
1	Elevation	0.707	-0.486	0.140	0.062	-0.354	-0.393	0.351
1	Slope	0.803	0.232	-0.363	-0.206	0.164	0.254	-0.029
climate								
2	MAT	-0.178	0.967	-0.820	-0.145	0.743	0.581	-0.411
2	MAP	-0.065	0.966	-0.806	-0.262	0.800	0.799	-0.438
season								
3	PS	-0.011	-0.603	0.833	0.127	-0.374	-0.508	0.260
3	TS	-0.251	-0.852	0.936	0.252	-0.679	-0.616	0.307
texture								
4	Clay	0.125	0.267	-0.261	-0.952	0.246	0.449	0.026
4	Sand	-0.035	-0.002	0.063	0.723	0.029	-0.220	-0.062
soil								
5	GPP	-0.123	0.822	-0.620	-0.114	0.917	0.525	-0.345
5	BGB	0.112	0.182	-0.234	-0.308	0.491	0.536	-0.286
5	Shannon_EVI	0.268	-0.250	0.076	-0.258	-0.212	-0.030	0.180
vegetation								
6	BD	-0.286	0.360	-0.232	-0.058	0.205	0.240	-0.049
6	pH	0.021	-0.687	0.632	0.432	-0.653	-0.993	0.535
6	Moisture	0.039	0.032	-0.091	-0.028	-0.004	0.033	0.041
CUE								
7	CUE	0.191	-0.439	0.322	-0.042	-0.434	-0.534	1.000

INNER MODEL

$climate				
	Estimate	Std. Error	t value	Pr(>|t|)
Intercept	-3.60e-16	0.051	-7.05e-15	1.00e+00
topography	-1.27e-01	0.051	-2.48e+00	0.014
$season				
	Estimate	Std. Error	t value	Pr(>|t|)
Intercept	3.17e-16	0.024	1.35e-14	1.00e+00
topography	-2.87e-01	0.024	-1.21e+01	1.40e-28
climate	-8.79e-01	0.024	-3.70e+01	2.81e-127
$texture				
	Estimate	Std. Error	t value	Pr(>|t|)
Intercept	3.59e-17	0.050	7.16e-16	1.00e+00
topography	-7.21e-02	0.051	-1.42e+00	0.157
season	2.15e-01	0.051	4.22e+00	0.000
$vegetation				

	Estimate	Std. Error	t value	Pr(>|t|)
Intercept	3.64e-16	0.031	1.18e-14	1.00e+00
climate	9.34e-01	0.057	1.64e+01	8.19e-46
season	1.62e-01	0.057	2.83e+00	4.85e-03
$soil				
	Estimate	Std. Error	t value	Pr(>|t|)
Intercept	1.41e-16	0.033	4.30e-15	1.00e+00
season	-3.17e-01	0.042	-7.49e+00	4.87e-13
texture	-2.81e-01	0.034	-8.36e+00	1.24e-15
vegetation	4.15e-01	0.042	9.89e+00	1.16e-20
$CUE				
	Estimate	Std. Error	t value	Pr(>|t|)
Intercept	5.03e-16	0.041	1.24e-14	1.00e+00
climate	-1.74e-01	0.101	-1.73e+00	8.47e-02
season	-1.90e-01	0.077	-2.48e+00	1.37e-02
texture	-3.16e-01	0.046	-6.94e+00	1.72e-11
vegetation	-5.10e-02	0.070	-7.27e-01	4.68e-01
soil	-6.33e-01	0.066	-9.66e+00	7.28e-20

CORRELATIONS BETWEEN LVs

	Topography	Climate	Season	Texture	Vegetation	Soil	CUE
Topography	1.000	-0.127	-0.176	-0.110	-0.096	-0.055	0.191
Climate	-0.127	1.000	-0.843	-0.210	0.798	0.713	-0.439
Season	-0.176	-0.843	1.000	0.227	-0.625	-0.641	0.322
Texture	-0.110	-0.210	0.227	1.000	-0.185	-0.429	-0.042
Vegetation	-0.096	0.798	-0.625	-0.184	1.000	0.665	-0.434
Soil	-0.055	0.713	-0.640	-0.429	0.665	1.000	-0.534
CUE	0.191	-0.439	0.322	-0.042	-0.434	-0.534	1.000

SUMMARY INNER MODEL

	Type	R_2	Block_Communality	Mean_Redundancy	AVE
Topography	Exogenous	0.000	0.573	0.000	0.573
Climate	Endogenous	0.016	0.933	0.015	0.933
Season	Endogenous	0.791	0.785	0.621	0.785
Clay	Endogenous	0.057	1.715	0.041	1.715
Soil	Endogenous	0.644	0.376	0.242	0.000
Vegetation	Endogenous	0.580	0.348	0.209	0.000
CUE	Endogenous	0.388	1.000	0.388	1.000

GOODNESS-OF-FIT
[1] 0.493

TOTAL EFFECTS

	relationships	direct	indirect	total
1	topography -> climate	-0.127	0.000	-0.127
2	topography -> season	-0.287	0.111	-0.176
3	topography -> clay	-0.072	-0.038	-0.110
4	topography -> vegetation	0.000	-0.147	-0.147
5	topography -> soil	0.000	0.026	0.026
6	topography -> CUE	0.000	0.081	0.082
7	climate -> season	-0.879	0.000	-0.879
8	climate -> texture	0.000	-0.189	-0.187
9	climate -> vegetation	0.934	-0.142	0.792

10	climate -> soil	0.000	0.660	0.660
11	climate -> CUE	-0.174	-0.232	-0.406
12	season -> texture	0.215	0.000	0.215
13	season -> vegetation	0.162	0.000	0.162
14	season -> soil	-0.317	0.007	-0.310
15	season -> CUE	-0.190	0.120	-0.070
16	texture -> vegetation	0.000	0.000	0.000
17	texture -> soil	-0.281	0.000	-0.281
18	texture -> CUE	-0.316	0.178	-0.138
19	vegetation -> soil	0.415	0.000	0.415
20	vegetation -> CUE	-0.051	-0.263	-0.314
21	soil -> CUE	-0.633	0.000	-0.633

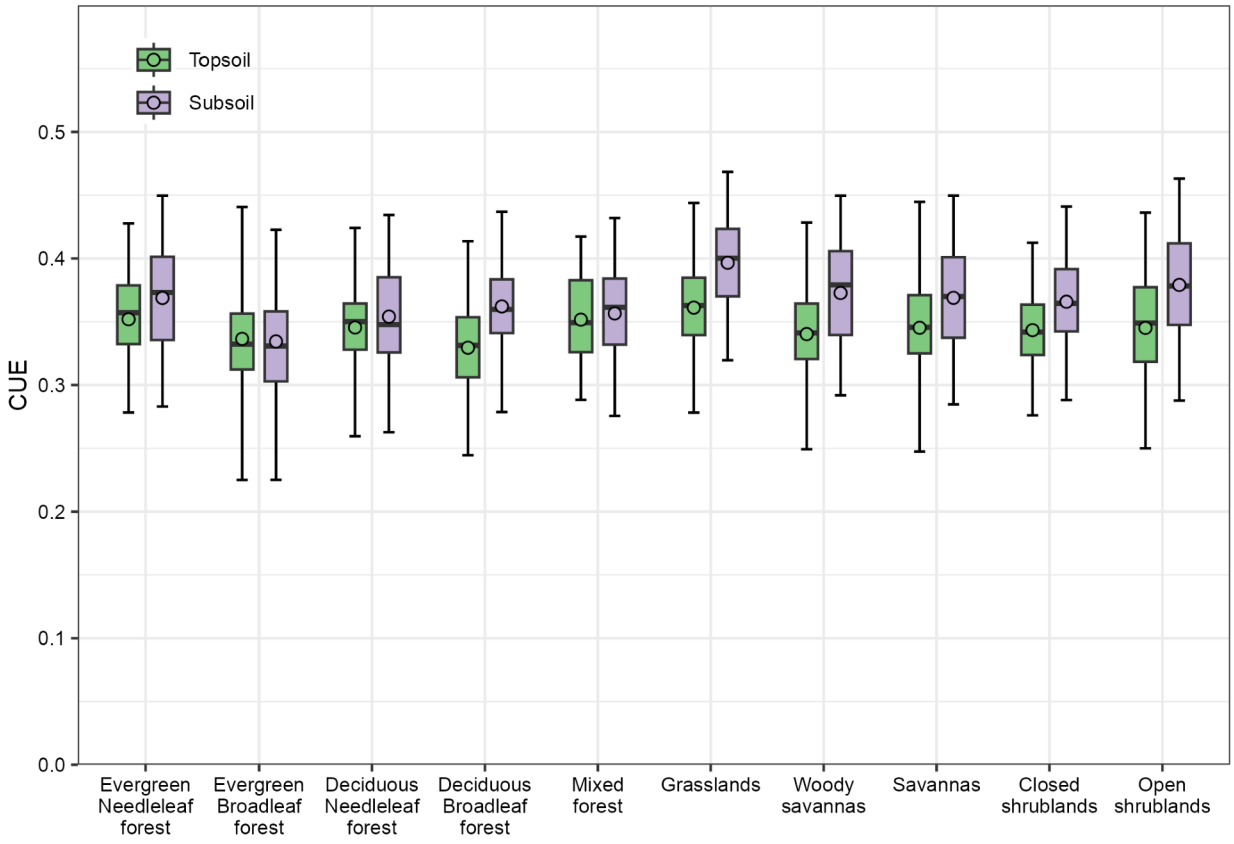

Fig. S5 CUE values across biomes in both topsoils and subsoils. The boxes represent the first and the third quartiles. The line within the box represents the median. The whiskers represent the data range and points indicate individual values. The biomes are delineated using MODIS land-cover maps.

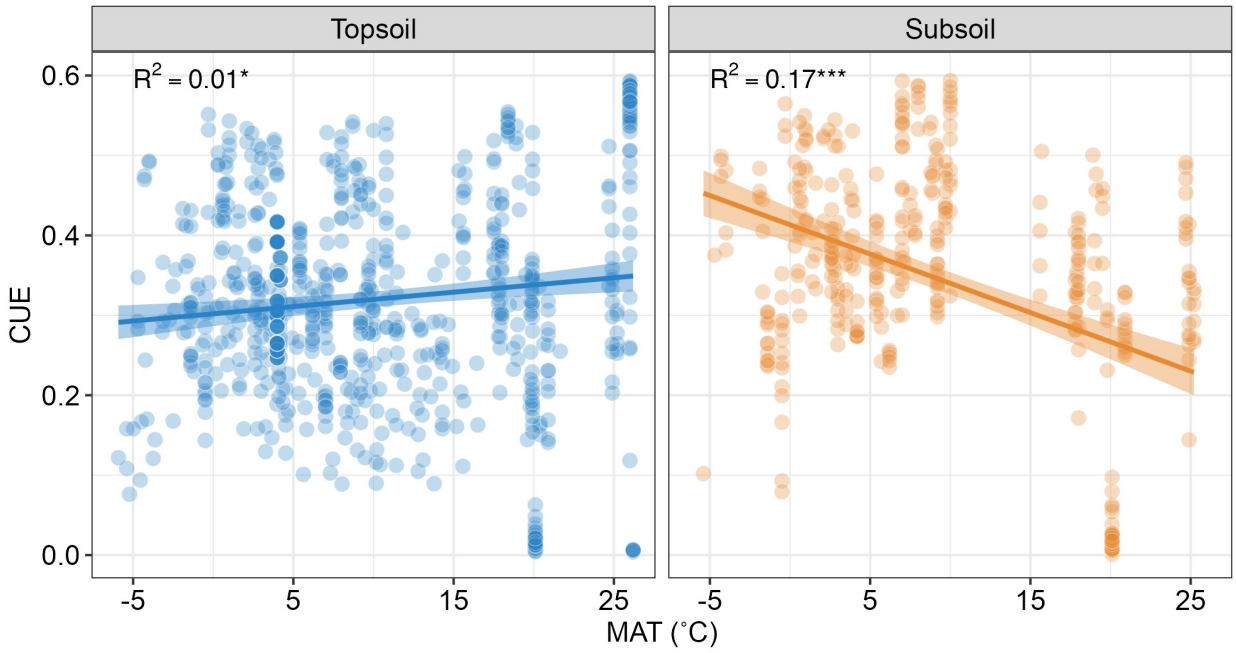

Fig. S6 Relationships between CUE and mean annual temperature (MAT). Linear regressions depicting the relationship between CUE and MAT in topsoils and in subsoils. The dots correspond to individual values (n=814 and 379 for topsoils and subsoils, respectively). * denotes $P < 0.05$; *** indicates $P < 0.001$.

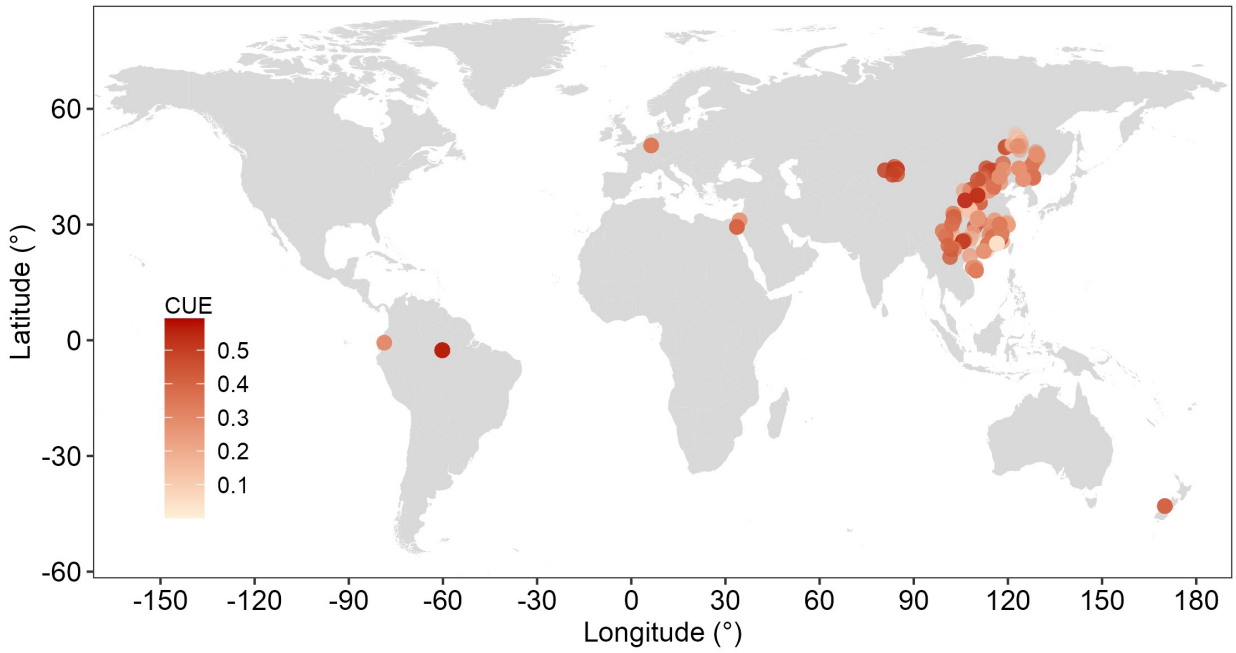

Fig. S7 Global distribution of microbial carbon use efficiency (CUE) estimated with stoichiometric modeling. In total, 1193 data points across 103 sites.

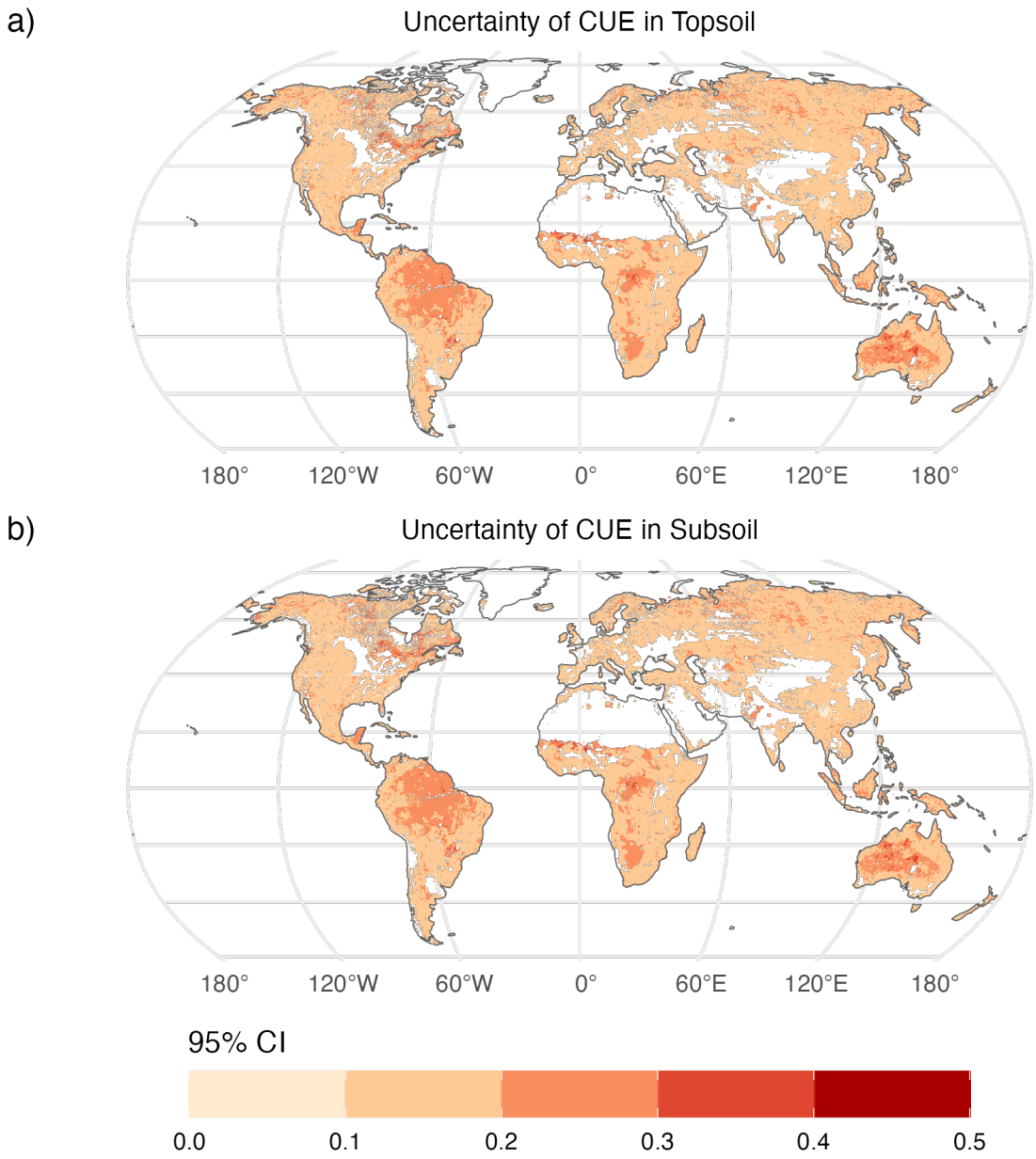

Fig. S8 Global distribution of the uncertainty of prediction of CUE in a) topsoil and b) subsoil. Uncertainty is calculated by mean value of 100 times model 95% confidence interval (CI). All projections are displayed on a 0.25˚ x 0.25˚ scale of latitude and longitude. Areas of water, permanent wetlands, cropland, urban/built-up areas, and snow/ice areas were excluded from projections.

Table S3 Description of data from 21 potential predictors of microbial carbon use efficiency (CUE)

Factors	ID	Variable	Unit	Source	Period/Layer	Reference
Climate	1	Mean annual temperature (MAT)	°C	WorldClim2	1970-2000	Fick and Hijmans, 2017
	2	Mean annual precipitation (MAP)	mm	WorldClim2	1970-2000	Fick and Hijmans, 2017
	3	Temperature seasonality (TS)	10^{-2} °C	WorldClim2	1970-2000	Fick and Hijmans, 2017
	4	Precipitation seasonality (PS)	%	WorldClim2	1970-2000	Fick and Hijmans, 2017
	5	Aridity index (AI)	-	global-aridity-index-and-potential-evapotranspiration-climate-database-v2/	1970-2000	Trabucco and Zomer, 2018
Vegetation	6	Shannon diversity enhanced vegetation index (EVI)	-	http://www.earthenv.org/texture	-	Tuanmu and Jetz, 2015
	7	Leaf area index (LAI)	m^2 m^{-2}	https://daac.ornl.gov/cgi-bin/dsviewer.pl?ds_id=1653	1981-2015	Mao and Yan, 2019
	8	Gross primary production (GPP)	g C m^{-2} d^{-1}	https://daac.ornl.gov/cgi-bin/dsviewer.pl?ds_id=1789	1982-2016	Madani and Parazoo, 2020
	9	Aboveground biomass (AGB)	Mg C ha^{-1}	https://daac.ornl.gov/VEGETATION/guides/Global_Maps_C_Density_2010.html	2010	Spawn et al., 2020
	10	Belowground biomass (BGB)	Mg C ha^{-1}	https://daac.ornl.gov/VEGETATION/guides/Global_Maps_C_Density_2010.html	2010	Spawn et al., 2020
	11	Root depth	m	https://wci.earth2observe.eu/thredds/catalog/usc/root-depth/catalog.html	-	Fan et al., 2017
Topography	12	Elevation	m	http://www.earthenv.org/topography	-	Amatulli et al., 2018
	13	Slope	degrees	http://www.earthenv.org/topography	-	Amatulli et al., 2018
Soil	14	Depth to bedrock	cm (≤ 200)	https://files.isric.org/soilgrids/former/2017-03-10/data/	-	Hengl et al., 2017
	15	Soil clay fraction	% of weight	http://globalchange.bnu.edu.cn/research/soilw#download	0-100 cm	
	16	Soil silt fraction	% of weight	http://globalchange.bnu.edu.cn/research/soilw#download	0-100 cm	
	17	Soil sand fraction	% of weight	http://globalchange.bnu.edu.cn/research/soilw#download	0-100 cm	
	18	Soil bulk density (BD)	g cm^{-3}	http://globalchange.bnu.edu.cn/research/soilw#download	0-100 cm	
	19	Soil moisture	% of volume	http://globalchange.bnu.edu.cn/research/soilw#download	0-100 cm	
	20	Cation exchange capacity (CEC)	cmol kg^{-1}	http://globalchange.bnu.edu.cn/research/soilw#download	0-100 cm	
	21	pH in H_2O	-	http://globalchange.bnu.edu.cn/research/soilw#download	0-100 cm	

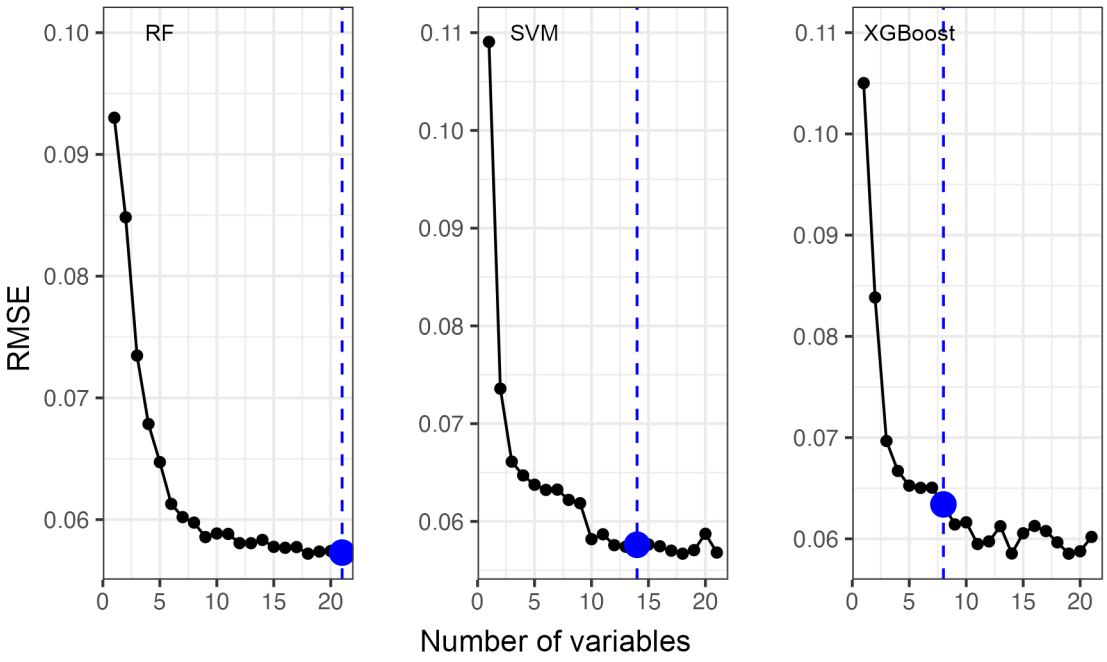

Fig. S9 Results of the recursive feature elimination method in topsoils, which was used to prevent the overfitting of the Random Forest (RF) model, Support Vector Machine (SVM), and Extreme Gradient-Boosting (XGBoost) model in predicting microbial carbon use efficiency (CUE). Blue dots and lines represent the optimal numbers of predictor variables used to train machine-learning models. RMSE denotes the root mean square error.

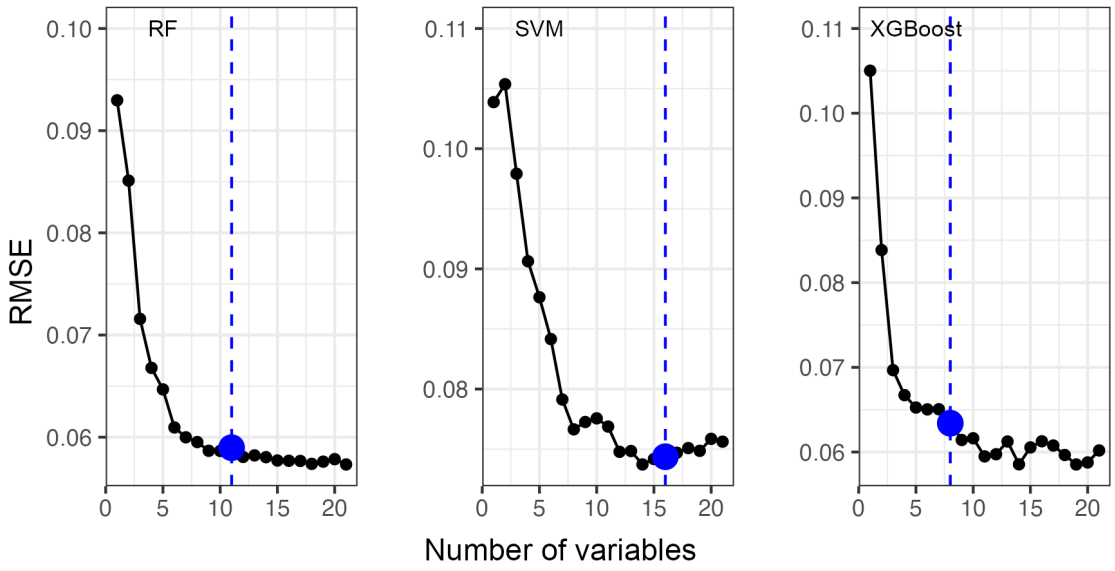

Fig. S10 Results of the recursive feature elimination method in subsoils, which was used to prevent the overfitting of the Random Forest (RF) model, Support Vector Machine (SVM), and Extreme Gradient-Boosting (XGBoost) model in predicting microbial carbon use efficiency (CUE). Blue dots and lines represent the optimal numbers of predictor variables used to train machine-learning models. RMSE denotes the root mean square error.

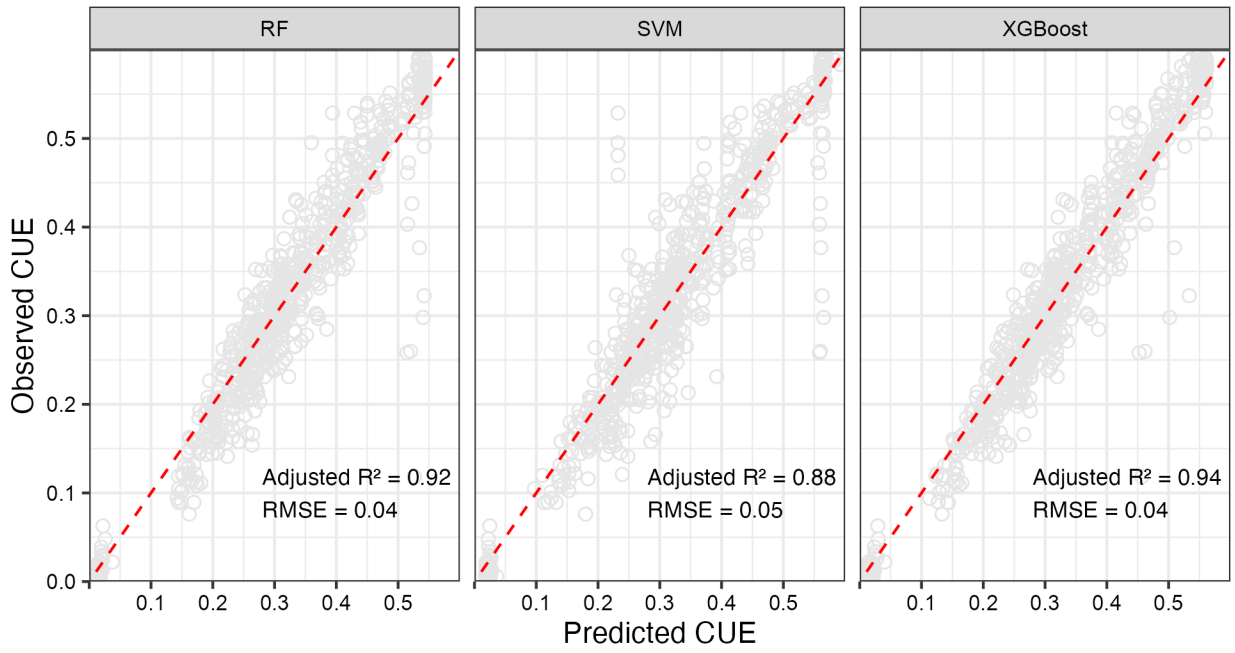

Fig. S11 Performance of the Random Forest (RF) model, Support Vector Machine (SVM), and Extreme Gradient-Boosting (XGBoost) model in predicting microbial carbon use efficiency (CUE) in topsoils. The red dashed lines represent the 1:1 line. Adjusted R^2 indicates the coefficient of determination. RMSE denotes the root mean squared error. The optimal model is characterized by the maximum R^2 and the minimum RMSE.

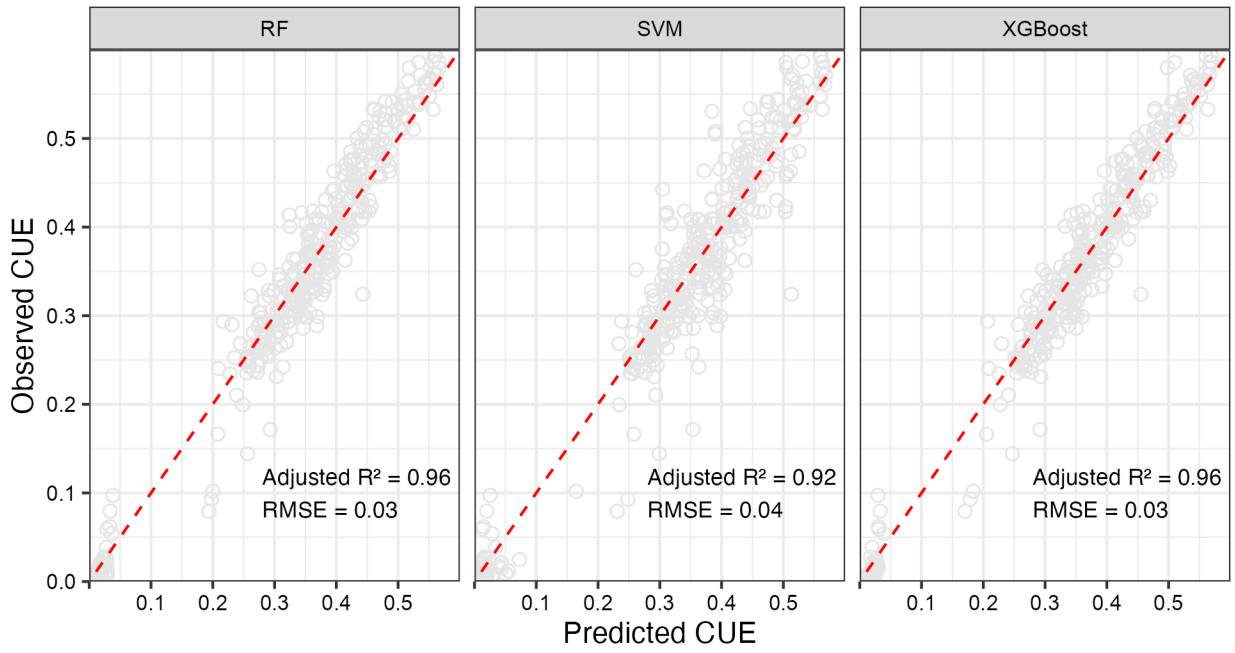

Fig. S12 Performance of the Random Forest (RF) model, Support Vector Machine (SVM), and Extreme Gradient-Boosting (XGBoost) model in predicting microbial carbon use efficiency (CUE) in subsoils. The red dashed lines represent the 1:1 line. Adjusted R^2 indicates the coefficient of determination. RMSE denotes the root mean squared error. The optimal model is characterized by the maximum R^2 and the minimum RMSE.

Table S4 Results of recursive feature elimination method in subsoils, which was used to prevent the overfitting of the Random Forest (RF) model, support vector machine (SVM) model, Extreme Gradient-Boosting (XGBoost) model in predicting microbial carbon use efficiency (CUE) in topsoils

Explanatory variables	RF	SVM	XGBoost
Mean annual temperature (MAT)	√	√	√
Mean annual precipitation (MAP)	√	√	√
Temperature seasonality (TS)	√	√	√
Precipitation seasonality (PS)	√	√	√
Aridity index (AI)	√	√	√
Elevation	√	√	√
Slope	√	√	√
pH	√	√	√
Soil moisture	√	√	√
Soil bulk density (BD)	√	√	√
Cation exchange capacity (CEC)	√	√	√
Soil sand content	√	√	√
Soil clay content	√	√	√
soil silt content	√	√	√
RootDepth	√	√	
Bedrock	√	√	√
Aboveground biomass (AGB)	√	√	√
Belowground biomass (BGB)	√	√	√
Leaf area index (LAI)	√	√	√
Shannon enhanced vegetation index	√	√	√
Gross primary production (GPP)	√	√	
Adjust R^2	0.92	0.88	0.94
RMSE	0.04	0.05	0.04

Table S5 Results of recursive feature elimination method in subsoils, which was used to prevent the overfitting of the Random Forest (RF) model, support vector machine (SVM) model, Extreme Gradient-Boosting (XGBoost) model in predicting microbial carbon use efficiency (CUE) in subsoils

Explanatory variables	RF	SVM	XGBoost
Mean annual temperature (MAT)	√	√	√
Mean annual precipitation (MAP)	√	√	
Temperature seasonality (TS)	√	√	√
Precipitation seasonality (PS)		√	
Aridity index (AI)		√	
Elevation		√	√
Slope	√		
pH	√	√	√
Soil moisture	√		
Soil bulk density (BD)		√	
Cation exchange capacity (CEC)	√	√	√
Soil sand content	√	√	
Soil clay content	√		√
soil silt content		√	
RootDepth			
Bedrock		√	
Aboveground biomass (AGB)		√	√
Belowground biomass (BGB)		√	
Leaf area index (LAI)	√	√	√
Shannon enhanced vegetation index	√	√	
Gross primary production (GPP)			
Adjust R^2	0.96	0.92	0.96
RMSE	0.03	0.04	0.03

Supplementary References:

Amatulli, G, Domisch, S, Tuanmu, M-N, Parmentier, B, Ranipeta, A, Malczyk, J, Jetz, W, 2018. A suite of global, cross-scale topographic variables for environmental and biodiversity modeling. Scientific Data 5, 180040. https://doi.org/10.1038/sdata.2018.40

Chen, L, Xue, Y, Wang, N, Gao, H, Hu, G, Liu, J e, Cao, L, Zhou, Z, 2025. Soil properties influence the distribution and diversity of plant communities in the desert-loess transition zone. CATENA 254, 108976. https://doi.org/10.1016/j.catena.2025.108976

Churkina, G, Running, S W, 1998. Contrasting Climatic Controls on the Estimated Productivity of Global Terrestrial Biomes. Ecosystems 1, 206-215. https://doi.org/10.1007/s100219900016

Cui, Y, Peng, S, Rillig, M C, Camenzind, T, Delgado-Baquerizo, M, Terrer, C, Xu, X, et al., 2025. Global patterns of nutrient limitation in soil microorganisms. Proceedings of the National Academy of Sciences 122, e2424552122. https://doi.org/10.1073/pnas.2424552122

Daly, C, Halbleib, M, Smith, J I, Gibson, W P, Doggett, M K, Taylor, G H, Curtis, J, Pasteris, P P, 2008. Physiographically sensitive mapping of climatological temperature and precipitation across the conterminous United States. International Journal of Climatology 28, 2031-2064. https://doi.org/10.1002/joc.1688

Daniels, W L, 2016. The Nature and Properties of Soils, 15th Edition Ray R. Weil and Nyle C. Brady. Pearson Press, Upper Saddle River NJ, 2017. 1086 p. $164.80. ISBN-

10: 0-13-325448-8; ISBN-13: 978-0-13-325448-8. Also available as eText for $67.99. Soil Science Society of America Journal 80, 1428-1428. https://doi.org/10.2136/sssaj2016.0005br

Domeignoz-Horta, L A, Cappelli, S L, Shrestha, R, Gerin, S, Lohila, A K, Heinonsalo, J, Nelson, D B, et al., 2024. Plant diversity drives positive microbial associations in the rhizosphere enhancing carbon use efficiency in agricultural soils. Nature Communications 15, 8065. https://doi.org/10.1038/s41467-024-52449-5

Fan, Y, Miguez-Macho, G, Jobbágy, E G, Jackson, R B, Otero-Casal, C, 2017. Hydrologic regulation of plant rooting depth. Proceedings of the National Academy of Sciences 114, 10572-10577. https://doi.org/10.1073/pnas.1712381114

Fick, S E, Hijmans, R J, 2017. WorldClim 2: new 1-km spatial resolution climate surfaces for global land areas. International Journal of Climatology 37, 4302-4315. https://doi.org/10.1002/joc.5086

Hajek, O L, Knapp, A K, 2022. Shifting seasonal patterns of water availability: ecosystem responses to an unappreciated dimension of climate change. New Phytologist 233, 119-125. https://doi.org/10.1111/nph.17728

Han, W, Chen, L, Su, X, Liu, D, Jin, T, Shi, S, Li, T, Liu, G, 2022. Effects of Soil Physico-Chemical Properties on Plant Species Diversity Along an Elevation Gradient Over Alpine Grassland on the Qinghai-Tibetan Plateau, China. Frontiers in Plant Science Volume 13 - 2022, https://doi.org/10.3389/fpls.2022.822268

He, Y, Wang, X, Wang, K, Tang, S, Xu, H, Chen, A, Ciais, P, Li, X, Peñuelas, J, Piao, S, 2021. Data-driven estimates of global litter production imply slower vegetation carbon turnover. Global Change Biology 27, 1678-1688. https://doi.org/10.1111/gcb.15515

Helman, D, Osem, Y, Yakir, D, Lensky, I M, 2017. Relationships between climate, topography, water use and productivity in two key Mediterranean forest types with different water-use strategies. Agricultural and Forest Meteorology 232, 319-330. https://doi.org/10.1016/j.agrformet.2016.08.018

Hengl, T, Mendes de Jesus, J, Heuvelink, G B M, Ruiperez Gonzalez, M, Kilibarda, M, Blagotić, A, Shangguan, W, et al., 2017. SoilGrids250m: Global gridded soil information based on machine learning. PLOS ONE 12, e0169748. https://doi.org/10.1371/journal.pone.0169748

Luo, Z, Wang, G, Wang, E, 2019. Global subsoil organic carbon turnover times dominantly controlled by soil properties rather than climate. Nature Communications 10, 3688. https://doi.org/10.1038/s41467-019-11597-9

Mackie-Dawson, L A, Mullins, C E, Goss, M J, Court, M N, Fitzpatrick, E A, 1989. Seasonal changes in the structure of clay soils in relation to soil management and crop type. II. Effects of cultivation and cropping at Compton Beauchamp. Journal of Soil Science 40, 283-292. https://doi.org/10.1111/j.1365-2389.1989.tb01273.x

Manzoni, S, Taylor, P, Richter, A, Porporato, A, Ågren, G I, 2012. Environmental and stoichiometric controls on microbial carbon-use efficiency in soils. New Phytologist 196, 79-91. https://doi.org/10.1111/j.1469-8137.2012.04225.x

Mao, J, Yan, B, 2019. Global Monthly Mean Leaf Area Index Climatology, 1981-2015 (Version 1). ORNL Distributed Active Archive Center https://doi.org/10.3334/ORNLDAAC/1653

Moustakis, Y, Onof, C J, Paschalis, A, 2020. Atmospheric convection, dynamics and topography shape the scaling pattern of hourly rainfall extremes with temperature globally. Communications Earth & Environment 1, 11. https://doi.org/10.1038/s43247-020-0003-0

Peel, M C, Finlayson, B L, McMahon, T A, 2007. Updated world map of the Köppen-Geiger climate classification. Hydrol. Earth Syst. Sci. 11, 1633-1644. https://doi.org/10.5194/hess-11-1633-2007

Potter, C, Boriah, S, Steinbach, M, Kumar, V, Klooster, S, 2008. Terrestrial vegetation dynamics and global climate controls. Climate Dynamics 31, 67-78. https://doi.org/10.1007/s00382-007-0339-5

R. C, C, 1941. Factors of Soil Formation, a System of Quantitative Pedology. Agronomy Journal 33, 857-858. https://doi.org/10.2134/agronj1941.00021962003300090016x

Roe, G H, 2005. OROGRAPHIC PRECIPITATION. Annual Review of Earth and Planetary Sciences 33, 645-671. https://doi.org/10.1146/annurev.earth.33.092203.122541

Sarkar, S, Das, D K, Singh, A, Laik, R, Singh, S K, van Es, H M, Krishnan, K, et al., 2024. Seasonal variations in soil characteristics control microbial respiration and carbon

use under tree plantations in the middle gangetic region. Heliyon 10, e35593. https://doi.org/10.1016/j.heliyon.2024.e35593

Soinne, H, Keskinen, R, Tähtikarhu, M, Kuva, J, Hyväluoma, J, 2023. Effects of organic carbon and clay contents on structure-related properties of arable soils with high clay content. European Journal of Soil Science 74, e13424. https://doi.org/10.1111/ejss.13424

Spawn, S A, Gibbs, H K, 2020. Global Aboveground and Belowground Biomass Carbon Density Maps for the Year 2010 (Version 1). ORNL Distributed Active Archive Center https://doi.org/10.3334/ORNLDAAC/1763

Tuanmu, M-N, Jetz, W, 2015. A global, remote sensing-based characterization of terrestrial habitat heterogeneity for biodiversity and ecosystem modelling. Global Ecology and Biogeography 24, 1329-1339. https://doi.org/10.1111/geb.12365

Wuest, S B, 2015. Seasonal Variation in Soil Bulk Density, Organic Nitrogen, Available Phosphorus, and pH. Soil Science Society of America Journal 79, 1188-1197. https://doi.org/10.2136/sssaj2015.02.0066

Yao, Z, Xin, Y, Yang, L, Zhao, L, Ali, A, 2022. Precipitation and temperature regulate species diversity, plant coverage and aboveground biomass through opposing mechanisms in large-scale grasslands. Frontiers in Plant Science Volume 13 - 2022, https://doi.org/10.3389/fpls.2022.999636

Zhang, X, Zhang, W-C, Wu, W, Liu, H-B, 2023. Horizontal and vertical variation of soil clay content and its controlling factors in China. Science of The Total Environment 864, 161141. https://doi.org/10.1016/j.scitotenv.2022.161141

Zhang, Z, Li, X, Ju, W, Zhou, Y, Cheng, X, 2022. Improved estimation of global gross primary productivity during 1981–2020 using the optimized P model. Science of The Total Environment 838, 156172. https://doi.org/10.1016/j.scitotenv.2022.156172

Zomer, R J, Xu, J, Trabucco, A, 2022. Version 3 of the Global Aridity Index and Potential Evapotranspiration Database. Scientific Data 9, 409. https://doi.org/10.1038/s41597-022-01493-1